MONOLITHIC PHASE-LOCKED LOOPS AND CLOCK RECOVERY CIRCUITS

Theory and Design

edited by
BEHZAD RAZAVI

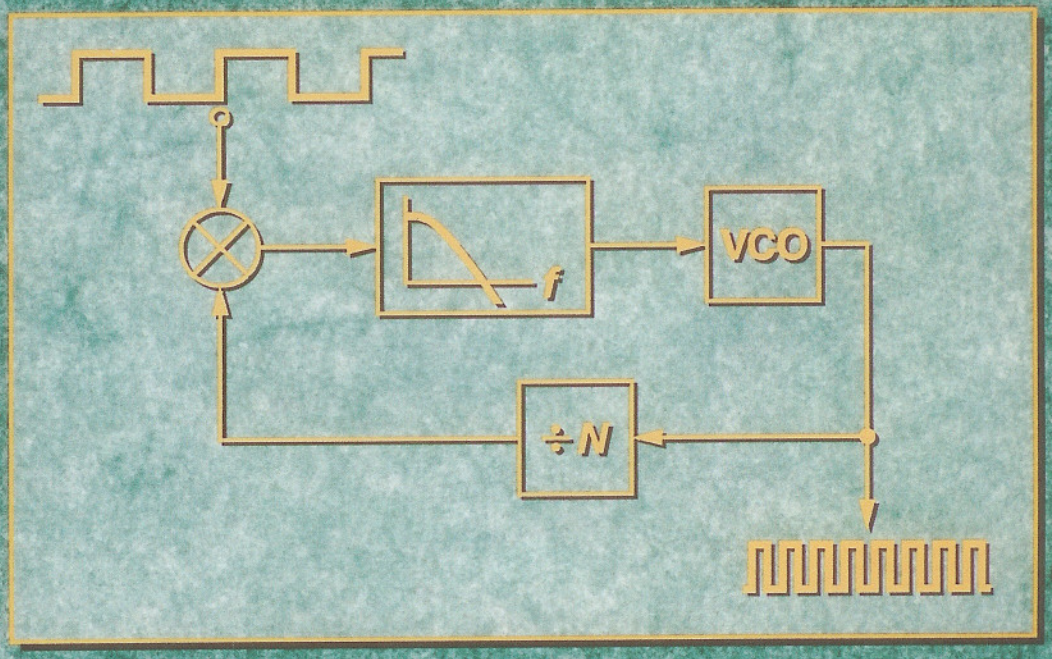

IEEE
PRESS

PART 2 BUILDING BLOCKS 199

Start-up and Frequency Stability in High-Frequency Oscillators . . . 201
N. M. Nguyen and R. G. Meyer (*IEEE Journal of Solid-State Circuits,* May 1992).
MOS Oscillators with Multi-Decade Tuning Range and Gigahertz Maximum Speed . . . 211
M. Banu (*IEEE Journal of Solid-State Circuits,* April 1988).
A Bipolar 1 GHz Multi-Decade Monolithic Variable-Frequency Oscillator . . . 219
J. T. Wu (*International Solid-State Circuit Conference Digest of Technical Papers,* February 1991).
A Digital Phase and Frequency Sensitive Detector . . . 222
J. I. Brown (*Proceedings of the IEEE,* April 1971).
A 3-State Phase Detector Can Improve Your Next PLL Design . . . 224
C. A. Sharpe (*EDN* Magazine, September 1976).
GaAs Monolithic Phase/Frequency Discriminator . . . 229
I. Shahriary et al. (*IEEE Gallium Arsenide Integrated Circuits Symposium Digest of Technical Papers,* October 1985).
A New Phase-Locked Loop Timing Recovery Method for Digital Regenerators . . . 233
J. A. Bellisio (*IEEE International Communications Conference Recording,* June 1976).
A Phase-Locked Loop with Digital Frequency Comparator for Timing Signal Recovery . . . 237
J. A. Afonso, A. J. Quiterio, and D. S. Arantes (*National Telecommunications Conference Recording,* 1979).
Clock Recovery from Random Binary Signals . . . 242
J. D. H. Alexander (*Electronics Letters,* October 1975).
A Si Bipolar Phase and Frequency Detector IC for Clock Extraction up to 8 Gb/s . . . 244
A. Pottbacker, U. Langmann, and H. U. Schreiber (*IEEE Journal of Solid-State Circuits,* December 1992).
A Self-Correcting Clock Recovery Circuit . . . 249
C. R. Hogge (*IEEE Journal of Lightwave Technology,* December 1985).

PART 3 MODELING AND SIMULATION 253

An Integrated PLL Clock Generator for 275 MHz Graphic Displays . . . 255
G. Gutierrez and D. DeSimone (*Proceedings of the Custom Integrated Circuits Conference,* May 1990).
The Macro Modeling of Phase-Locked Loops for the SPICE Simulator . . . 259
M. Sitkowski (*IEEE Circuits and Devices Magazine,* March 1991).
Modeling and Simulation of an Analog Charge Pump Phase-Locked Loop . . . 264
S. Can and Y. E. Sahinkaya (*Simulation,* April 1988).
Mixed-Mode Simulation of Phase-Locked Loops . . . 270
B. A. A. Antao, F. M. El-Turky, and R. H. Leonowich (*Proceedings of the Custom Integrated Circuits Conference,* May 1993).
Behavioral Representation for VCO and Detectors in Phase-Lock Systems . . . 274
E. Liu and A. L. Sangiovanni-Vincentelli (*Proceedings of the Custom Integrated Circuits Conference,* May 1992).
Behavioral Simulation Techniques for Phase/Delay-Locked Systems . . . 278
A. Demir, E. Liu, and A. L. Sangiovanni-Vincentelli (*Proceedings of the Custom Integrated Circuits Conference,* May 1994).

PART 4 PHASE-LOCKED LOOPS 283

A Monolithic Phase-Locked Loop with Detection Processor . . . 285
E. N. Murthi (*IEEE Journal of Solid State Circuits,* February 1979).
A 200-MHz CMOS Phase-Locked Loop with Dual Phase Detectors . . . 292
K. M. Ware, H.-S. Lee, and C. G. Sodini (*IEEE Journal of Solid-State Circuits,* December 1989).
High-Frequency Phase-Locked Loops in Monolithic Bipolar Technology . . . 301
M. Soyuer and R. G. Meyer (*IEEE Journal of Solid-State Circuits,* June 1989).
A 6-GHz Integrated Phase-Locked Loop Using AlGaAs/GaAs Heterojunction Bipolar Transistors . . . 310
A. W. Buchwald, et al. (*IEEE Journal of Solid-State Circuits,* December 1992).

Modeling and simulation of an Analog Charge-Pump Phase Locked Loop

Sumer Can
Signetics Corporation
Linear LSI Division
Sunnyvale, California 94086

and

Yilmaz E. Sahinkaya
Lockheed
Palo Alto Research Laboratory
Palo Alto, California 94304

SUMER CAN was born in Koyulhisar, Turkey, on December 24, 1947. He received his Y.Muh. (M.Sc.) degree in electrical engineering from Istanbul Technical University (Turkey) and his M.A.Sc. degree in electrical engineering from the University of Toronto (Canada) in 1972 and 1977 respectively. He worked at the Istanbul Technical University (1972-1974) as an instructor and at the University of Toronto (1974-1978) as a graduate assistant. In 1978, he joined the industry and worked at Litton Systems (Canada) Ltd., National Semiconductor Corp., Sperry-Univac, and Magnetic Peripherals Inc. Since 1984, he has been employed by Signetics Corporation, Sunnyvale, California in Linear LSI Division as a member of technical staff. His interests are bipolar/MOS integrated circuit design, circuits and system simulation, nonlinear dynamics, and chaotic circuits. Mr. Can is the author of several technical publications and patent disclosures in the area of circuits and systems.

YILMAZ E. SAHINKAYA received his B.Tech and M.S. degrees in mechanical engineering from the Loughborough College of Technology (England) and the University of Michigan in 1961 and 1962 respectively. He received his Ph.D. in electrical engineering from CalTech in 1969. His industrial experience includes Allis Chalmers Research Labs (1962-1964), Jet Propulsion Labs (1968-1970), Control Data Corporation (1970-1974), Bimsa (1976-1977), Control Data Corporation (1977-1985), and Lockheed Palo Alto Research Laboratory (1985-present).

His specialty is the design and development of large and complex control systems using computer simulation methodology. His current interest is the design and development of intelligent control systems utilizing microprocessors. He has published many papers in national conferences and currently is preparing a textbook entitled, "Applied Computer Simulation for Control Engineers."

ABSTRACT

We describe a nonlinear computer simulation model of an Analog Charge-Pump Phase Locked Loop (ACP-PLL). Offsets of the Phase Detector and Analog Charge-Pump are modeled as disturbances to simulate their effects on the steady-state phase error of the loop.

An extensive computer simulation study is carried out for the design of an example Analog CP-PLL using the proposed nonlinear model and comparing it to the conventional linear model. Results demonstrate the linear model is not sufficient to fully analyze and predict the behaviour of the Analog CP-PLL.

INTRODUCTION

The Analog CP-PLL is an electronic control system whose simplified block diagram is in Figure 1. The s_R and s_O are applied to the inputs of the Phase Detector which produces an output voltage s_D corresponding to the phase difference of these two input signals. The Phase Detector is followed by an Analog Charge-Pump. It consists of a Transconductance Amplifier with a capacitor at its output, forming an integrator. Note that this analog charge-pump is different from the Charge-Pump described by Gardner (1980) which is basically made of a current source/sink driven by a sequential-logic phase/frequency detector. The output of the loop filter is amplified and applied to the input of the Voltage Controlled Oscillator (VCO). This in turn produces an output signal at a frequency corresponding to the change of control voltage v_B such that it reduces the phase difference between s_R and s_O.

The operational characteristics of the Analog CP-PLL (Figure 1) are

(1) When the reference frequency f_R equals VCO frequency f_O, there is a 90° phase angle between s_R and s_O ($\Phi_E = \Phi_D - 90° = 0$).

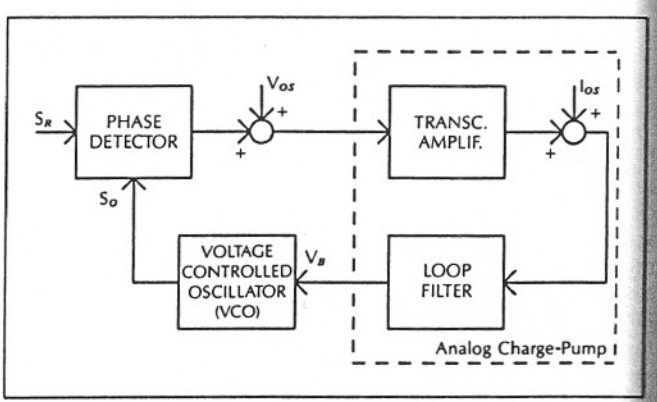

Figure 1. Analog Charge-Pump Phase Locked Loop (ACP-PLL).

Reprinted with permission from *Simulation*, S. Can and Y. E. Sahinkaya, "Modeling and Simulation of an Analog Charge Pump Phase-Locked Loop," vol. 50, pp. 155-160, April 1988.

(2) When the reference frequency changes to a new value, the VCO frequency takes up the same value within a required time interval, called "pull-in time" or "lock-in time." During this control action, the phase angle error ϕ_E, taken with respect to the 90° phase angle mentioned above, changes from zero to a positive or negative value and finally becomes zero when $f_R = f_O$ at the end of the pull-in time.

(3) When the reference frequency remains unchanged and a disturbance signal (i.e., V_{OS} and/or I_{OS}) enters into the system, the phase angle error changes from zero to a positive or negative value. The value of ϕ_E is proportional to the level of the offset signal.

The control action during the pull-in time is also known as the acquisition mode of operation. The control action, after frequency lock following a disturbance, is known as the tracking mode of operation. As in the following sections, all three major components of the Analog CP-PLL have nonlinearities.

Hence, the Analog CP-PLL is a nonlinear feedback control system whose system parameters and stability conditions which satisfy the prescribed performance requirements cannot be determined by well-known techniques such as "Root-Locus" and "Bode Plot" from the classical control theory. An efficient technique (Mitchell 1978; Dost and Liu 1985) to accomplish the task is use the power and flexibility of system simulation languages such as ACSL, CSSL-IV, or DSL/VS.

In this article, the usage of CSSL-IV is demonstrated in the determination of time-domain response characteristics of an example Analog CP-PLL.

The performance criteria of the Analog CP-PLL are set as:

(1) Settling time < 2 μs

(2) Overshoot < 20%

(3) Steady-state phase error < 3°

in response to the application of a 10% reference frequency step at f_R = 10 MHz; and Phase Detector offset V_{OS} = 10mV; and Charge-Pump offset I_{OS} = 75 μA in the form of step inputs.

MATHEMATICAL MODELING

Analog CP-PLL (see Figure 1) contains three main subcircuits: Phase Detector, Charge-Pump and Loop Filter, and Voltage Controlled Oscillator (VCO). We will briefly describe the operation of these subcircuits and present their mathematical models.

The main differences of this model from the classical models are that:

(1) The offsets of the Phase Detector and Charge-Pump are introduced into the model as disturbances.

(2) The Loop Filter is characterized with its state-space equations and used as a sub-block in the simulation.

Phase Detector: For a simplified circuit schematic of a typical analog phase detector see Figure 2. Apply the output of the VCO denoted by s_O to the upper transistor pairs Q3, Q4 and Q5, Q6. Apply the PLL's reference signal denoted by s_R to the lower transistor pair Q1, Q2. The input signals are given by:

$$s_R = A_R \sin(2\pi f_R t + \phi_R) \quad (1)$$

$$s_O = A_O \sin(2\pi f_O t + \phi_O) \quad (2)$$

where

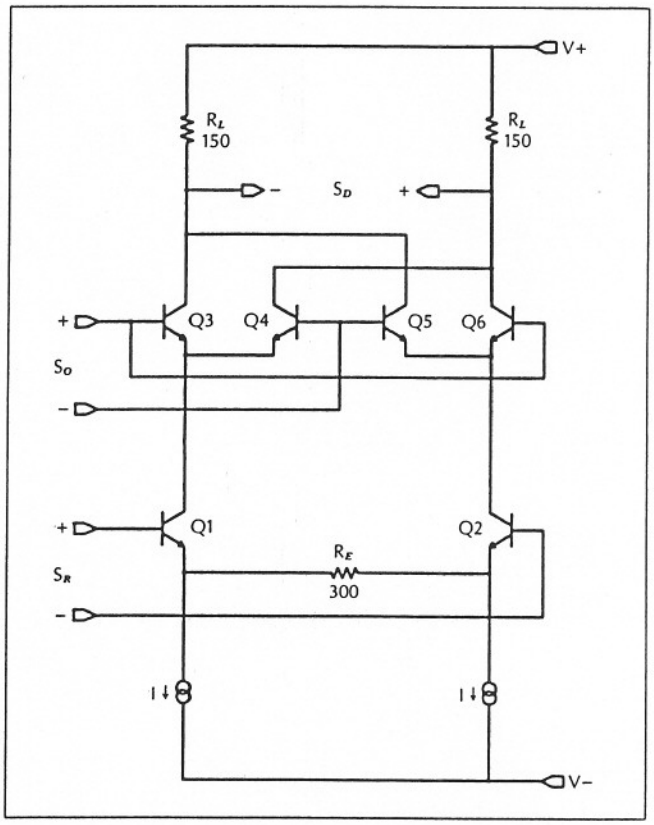

Figure 2. Simplified phase detector schematic.

A_R, A_O are the amplitudes; f_R, f_O are the frequencies and ϕ_R, ϕ_O are the phase angles of ACP-PLL's reference input and the VCO output, respectively.

An expression for the phase detector output signal S_D can be derived by observing its operational characteristics as follows:

- When s_R and s_O are in phase and have positive polarities, assume A_O is large enough so that transistors Q3, Q6 are fully turned "on" and transistors Q4, Q5 are fully turned "off." The differential pair Q1, Q2 and cascode transistors Q3, Q6 configuration yield a voltage of $s_D = (2R_L/R_E)s_R$ across load resistors R_L.
- When the input signals are in phase and have negative polarities, assume A_O is large enough so that transistors Q4, Q5 are fully turned "on" and transistors Q3, Q6 are fully turned "off." Since s_R is of negative polarity, differential pair Q1, Q2 and cascade transistors Q4, Q5 configuration yield a voltage of the same magnitude and polarity as in the previous case across load resistors R_L. Hence, the input reference signal is amplified. Also, its negative swinging half is inverted, producing an output signal s_D as a periodic function at twice the frequency of s_R with a maximum positive average dc level.
- When s_O lags s_R by 180°, using the same argument given above, s_D again is a similar periodic function with a maximum negative average dc level.
- When s_O lags s_R by 90°, s_D is a similar periodic function with a zero average dc level.
- When s_O lags s_R by any phase angle less than 90°, s_D is a periodic function with a positive average dc level. When s_O lags s_R by any phase angle more than 90°, s_D is a periodic function with a negative average dc level. In Figure 3 is the

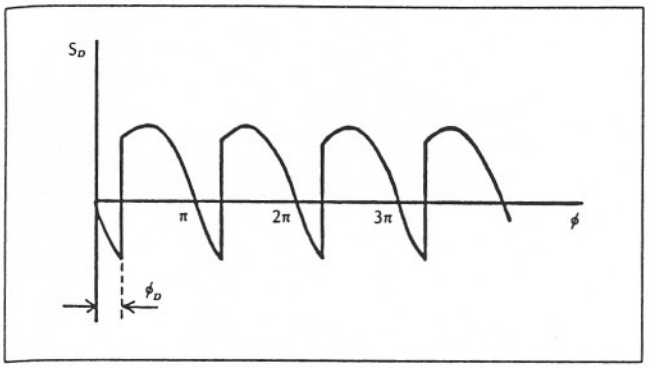

Figure 3. Phase detector output for a phase angle difference ϕ_D.

phase detector output signal s_D for a phase angle difference of ϕ_D between s_O and s_R.

Based on the above discussion an expression for s_D is given by:

$$s_D = (2R_L/R_E)\, s_R.\ \text{Sign}\{s_O\} \tag{3}$$

in which $(2R_L/R_E)$ is the dc gain of the phase detector, and Sign $\{s_O\}$ is defined by:

$$\text{Sign}\{s_O\} = +1 \qquad \text{for } s_O > 0 \tag{4a}$$

$$\text{Sign}\{s_O\} = 0 \qquad \text{for } s_O = 0 \tag{4b}$$

$$\text{Sign}\{s_O\} = -1 \qquad \text{for } s_O < 0 \tag{4c}$$

From Figure 3, an average value of s_D is given by:

$$s_D = (2R_L/\pi R_E)^*(\int_{\phi_o}^{\pi} A_R \text{Sin}\varphi\ d\varphi\ - \int_0^{\phi_o} A_R \text{Sin}\varphi\ d\varphi) \tag{5}$$

carrying out the integration in Eq. 5 yields:

$$s_D = (4R_L A_R/\pi R_E)\ \text{Cos}\phi_D \tag{6}$$

Since $\phi_E = \phi_D - 90°$, Eq. 6 can be rewritten as:

$$s_D = (4R_L A_R/\pi R_E)\ \text{Sin}\phi_E \tag{7}$$

Charge-Pump and Loop Filter: A simplified circuit schematic of an Analog Charge-Pump is in Figure 4. The differential output of the phase detector is applied to the input of differential pair Q1, Q2. The output current I_{CP} of this transconductance amplifier charges and discharges the capacitor C_{CP}. For $R_{CP} = 0$, the output current of the charge-pump is given by:

$$I_{CP} = I_{CS}\ \text{Tanh}\,(s_D/V_T) \tag{8}$$

where

I_{CS} is the constant current source; V_T is given by kT/q in which k is the Boltzmann constant, T is the absolute temperature, and q is the electronic charge. When $R_{CP} \neq 0$, the expression given in Eq. 8 can be simplified to a linear relationship as:

$$I_{CP} = (1/R_{CP})\ s_D \tag{9}$$

The Loop Filter forms by series connection of a resistor R_X and

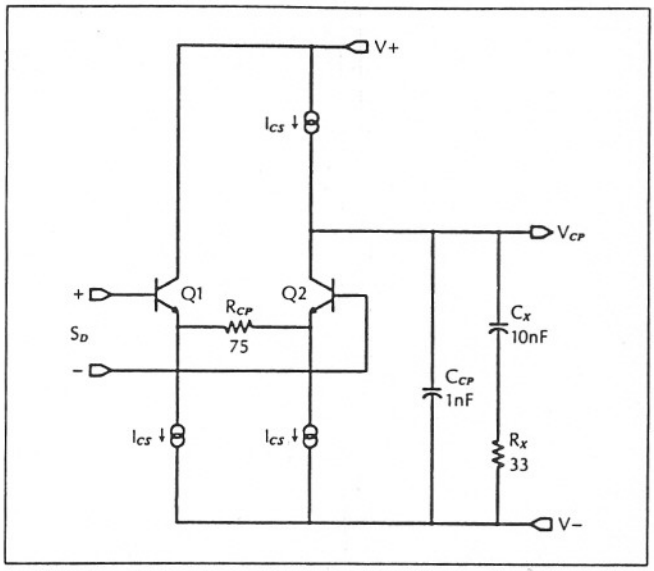

Figure 4. Simplified schematic of the Analog Charge-Pump and Loop Filter.

a capacitor C_X. The state equations for the configuration in Figure 4 are given by:

$$\dot{v}_{CP} = -[(b-1)/\tau]\, v_{CP} + [(b-1/\tau]\, v_{CX} + [(b-1)/C_X]\, I_{CP} \tag{10}$$

$$\dot{v}_{CX} = (1/\tau)\, v_{CP} - (1/\tau)\, v_{CX} \tag{11}$$

where

$\tau = R_X C_X;\ b = 1 + C_X/C_{CP}$.

Voltage Controlled Oscillator: A negative resistance LC type oscillator is considered as a VCO in this article. A simplified schematic of such oscillator is in Figure 5. The differential pair Q1, Q2 which is connected in a positive feedback configuration forms a negative resistor. The combination of an inductor L, a capacitor C_V and the negative resistor produces the oscillations at the collector of Q1. The amplitude of the oscillations is controlled by a subcircuit which varies the negative resistor by changing the tail current of differential pair Q1, Q2. The amplifier A drives a frequency divider circuit. The frequency of oscillation is given by:

$$f_O = K_D/2\pi[L\ C_V(v_B)]^{1/2} \tag{12}$$

where

K_D is coefficient introduced by the frequency divider ($K_D = 1/2$) circuit which follows the VCO and v_B is the output voltage of the buffer/amplifier following the charge-pump and is given by:

$$v_B = K_B\ v_{CP} \tag{13}$$

A voltage controlled capacitor (varactor) is used to realize frequency control by voltage. The capacitance C_V versus the buffer voltage v_B characteristic is nonlinear. However, the f_O versus v_B characteristic for a particular varactor used in our example is almost linear. Hence, Eq. 12 can be linearized and re-written as:

$$f_O = K_O\ v_B + f_{OC} \tag{14}$$

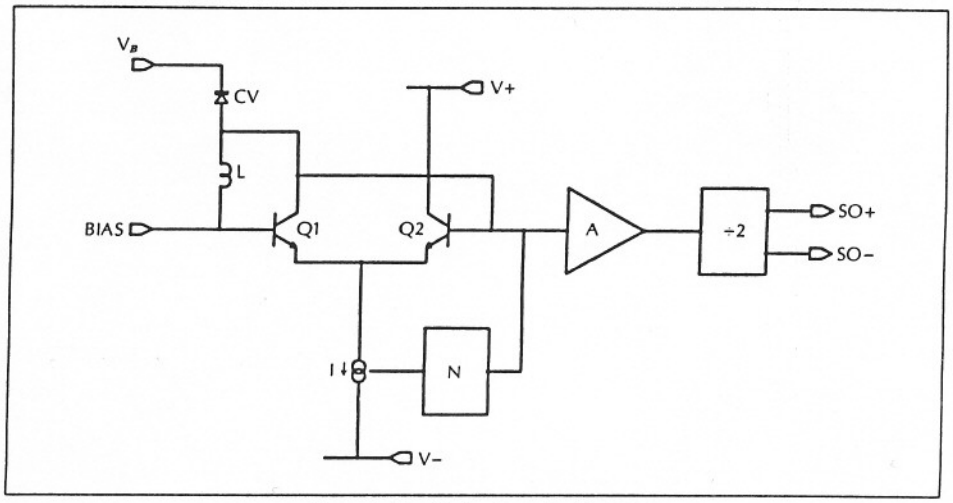

Figure 5. Simplified schematic of VCO.

where f_{OC} is the VCO's frequency of oscillation at $v_B = 0$, which is called center frequency (or free running frequency). Equation 14 is used in the linear analysis part of this study. The output of the VCO is given by:

$$s_O = A_O \sin[2\pi f_O(v_B)t + \phi_O(v_B)] \tag{15}$$

where

$$\dot{\phi}_O = f_O(v_B) \tag{16}$$

In Figure 6 is the complete block diagram corresponding to the nonlinear mathematical model developed for the Analog CP-PLL. Note that the offset voltage of the phase detector v_{OS} and the offset current of the charge-pump i_{OS} are introduced as disturbance signals in Figure 6.

COMPUTER SIMULATION

A computer simulation of the proposed Analog CP-PLL model is carried out in the following steps:

Step1. *Linear Analysis.* For small changes of ϕ_E, $Sin\phi_E$ is approximately equal to ϕ_E. Therefore, Eq. 7 can be linearized as:

$$s_D = (4R_L A_R/\pi R_E)\phi_E \tag{17}$$

Using linearized models of phase detector, transconductance amplifier and VCO given by Eqs. 17, 9, and 14 respectively, we obtain the block diagram of the linearized ACP-PLL as in Figure 7.

When the phase detector and charge-pump offsets are introduced into the system as $v_{OS} = v_{OS}\,u(t)$ and, $i_{OS} = I_{OS}\,u(t)$ where $u(t)$ being a unit step function, from the block diagram in Fig-

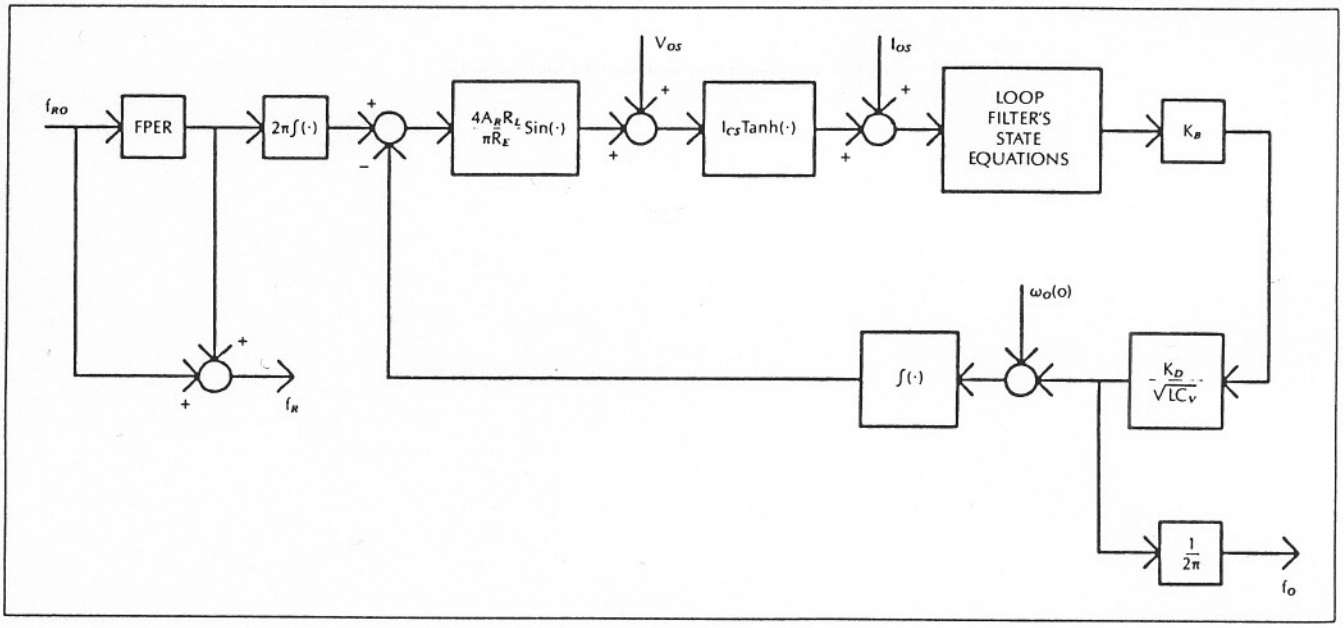

Figure 6. Simulation diagram of the nonlinear ACP-PLL.

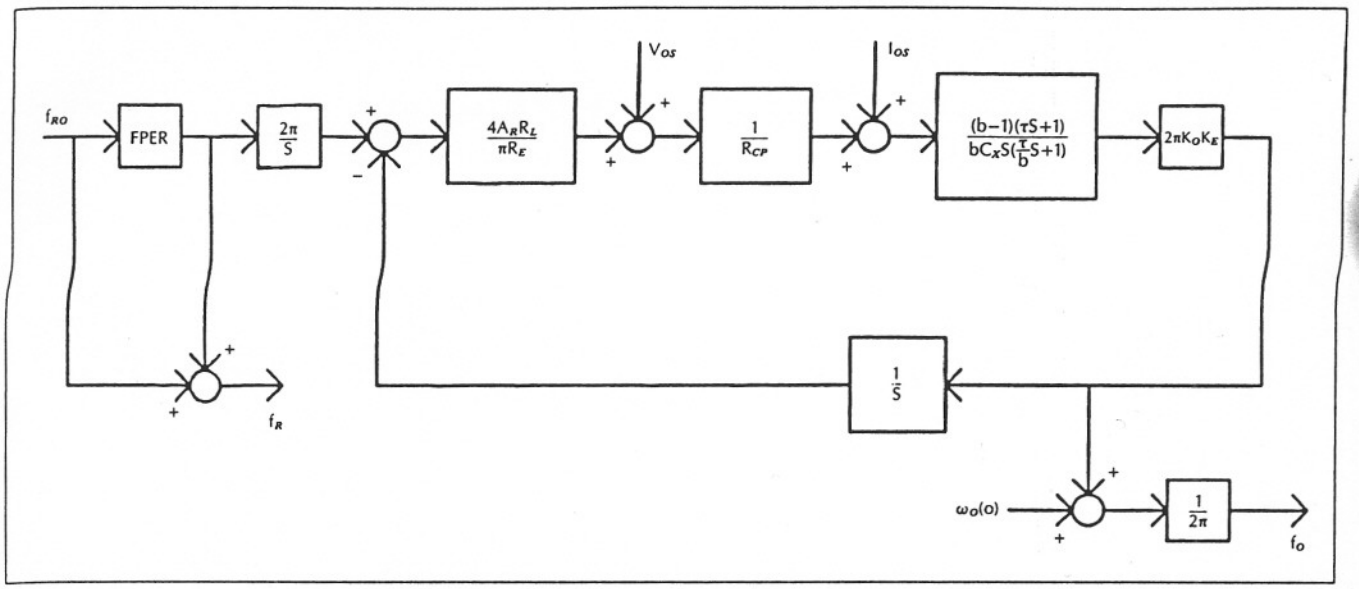

Figure 7. Simulation diagram of the linearized ACP-PLL.

ure 7, it can be shown that the steady-state phase error (Gardner 1979) due to offsets is:

$$\phi_e = (\pi R_E/4A_R R_L)[V_{OS} + R_{CP} I_{OS}] \quad (18)$$

From Figure 7, the closed-loop transfer function (when offsets are zero) is obtained as:

$$\phi_O/\phi_R = F(s)/[1 + F(s)] \quad (19)$$

where

$$F(s) = K(s + 1/\tau)/[s^2(s + b/\tau)] \quad (20)$$

in which

$$K = [8R_L A_R (b - 1) K_B K_O]/[R_E R_{CP} C_X] \quad (21)$$

$$\tau = R_X C_X \quad (22)$$

Substituting Eq. 20 into Eq. 19 we obtain:

$$\phi_O(s)/\phi_R(s) = K(s + \tau)/[s^3 + (b/\tau)s^2 + Ks + (K/\tau)] \quad (23)$$

where the characteristic equation is:

$$s^3 + (b/\tau)s^3 + Ks + (K/\tau) = 0 \quad (24)$$

The roots of Eq. 24 determine the response characteristics of the linear system as in Figure 7. Here, the system parameters used are $A_R = 0.2V$; $K_B = 2$; $K_O = 3.67 * 10^6$ Hz/V; $C_X = 10nF$; $R_X = 33$ ohm; $b = 11$; $R_L = 150$ ohm; $R_E = 300$ ohm. From the Root Locus diagram (not shown here) of Eq. 24, the roots of the characteristic equation and the gain which yield an acceptable system performance are determined. As a result, an initial value of 150 ohm is selected for the resistor, R_{CP}, of the linearized charge-pump.

A computer simulation program using CSSL-IV was developed (Can and Sahinkaya 1986) for the linear ACP-PLL and simulated for a 10% frequency step (i.e., *FPER* = 0.1) and zero offsets. The ACP-PLL response is in Figure 8a.

Step2. *Nonlinear Analysis.* A CSSL-IV program is also developed (Can and Sahinkaya 1986) for the nonlinear ACP-PLL model of Figure 6. The response of the nonlinear ACP-PLL for a same input frequency step as in linear ACP-PLL is in Figure 8b. From Figure 8, the following conclusions are drawn:

(1) The linear model *is not adequate* for predicting the response characteristics of the ACP-PLL.

(2) The "pull-in time" as predicted by the nonlinear model, with previously assumed circuit parameters, is about 14 μs which is about twice the value obtained from the linear model, and seven times larger than the maximum allowable value of 2 μs. Note that here, R_{CP} = 150 ohms. To reduce the "pull-in time" to an acceptable value, the loop gain must be increased without exceeding the stability limit. At this point, for the design method used in choosing the parameter values one may refer to a recent article by Gardner (1980).

Several computer runs have been made to optimize the design. Only the most interesting results are given here. The VCO frequency (see Figure 8b) loses its synchronism with the reference frequency for about 4 cycles before a "lock-in" is achieved. This clearly demonstrates the importance of the nonlinear analysis since the linear model will not show such characteristics. In Figure 9 is the response for final selection of parameter R_{CP} as 75 ohms for a frequency step of 10%.

In Figure 10 is the step response of the ACP-PLL when the linearized charge-pump model is replaced with the nonlinear model and other parameters are kept the same as in Figure 9. With the nonlinear charge-pump, the "lock-in" time is further reduced from approximately 5 μs (see Figure 9) to less than 2 μs.

CONCLUSIONS

A nonlinear mathematical model is developed for the simulation of Analog Charge-Pump Phase Locked Loops. Using CSSL-

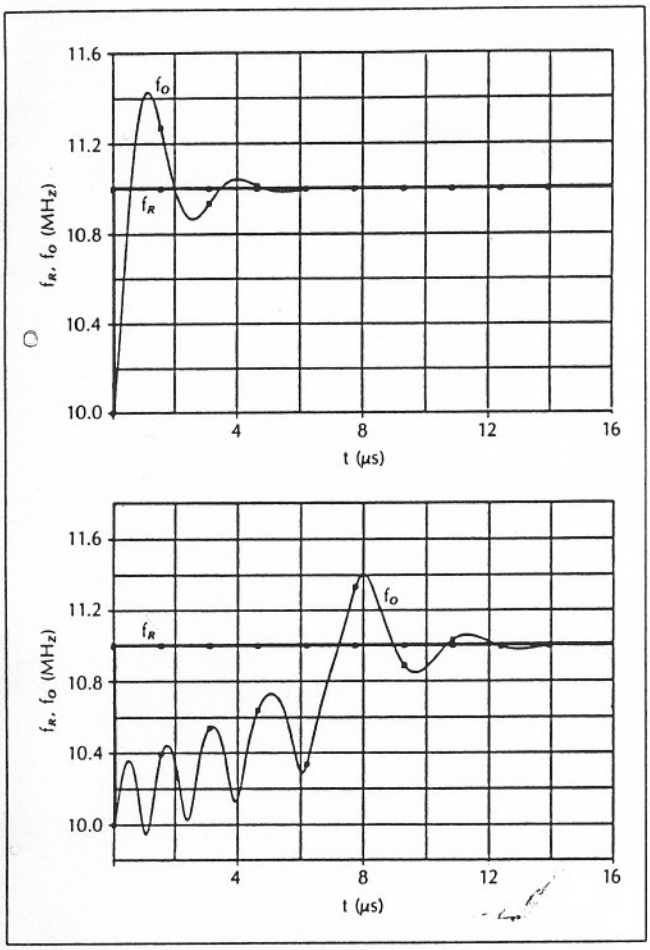

Figure 8. Step input response of (a) the linear ACP-PLL (R_{CP}=150Ω) (b) the nonlinear ACP-PLL with linear charge-pump (R_{CP}=150Ω).

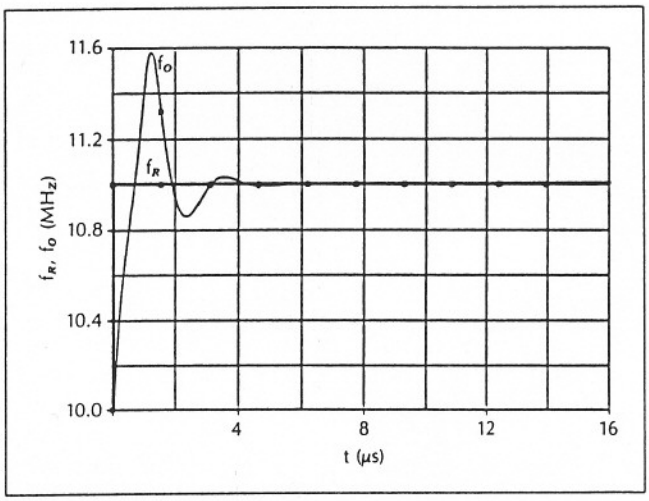

Figure 9. Step input response on nonlinear ACP-PLL with linear charge-pump (R_{CP}=75 ohms).

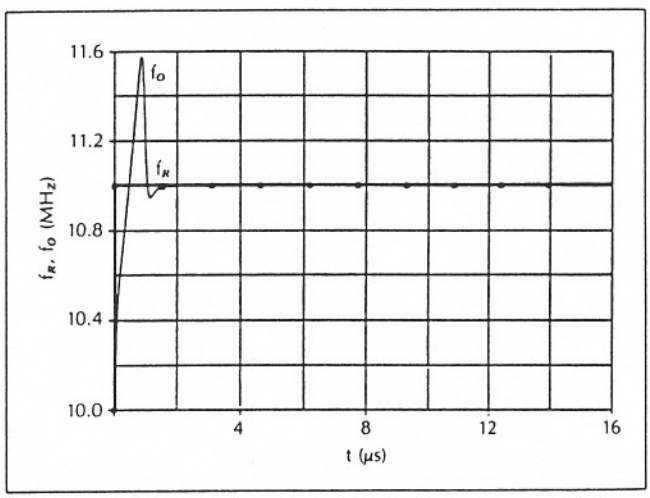

Figure 10. Step input response of nonlinear ACP-PLL with nonlinear charge-pump (R_{CP}=0).

IV, it was once again clearly shown that the linearized model is not sufficient to fully analyze and predict the response characteristics of the loop. It is almost mandatory to use computer based nonlinear analysis methodology for the design of Analog Charge-Pump Phase Locked Loops. The Phase Detector and Charge-Pump offsets are introduced as disturbances into the model and their influence on the ACP-PLL response characteristics is investigated.

REFERENCES

Can, S. and Y. E. Sahinkaya. 1986. "A Computer Simulation Model For An Analog Charge-Pump Phase Locked Loop." In *Proceedings of the 1986 Summer Computer Simulation Conference* (Reno, Nevada, July 28-30). SCS, San Diego, Calif., 886-892.

Dost, M. H. and C. C. Liu. 1985. "Variable Frequency Clock Study Using DSL/VS." In *Proceedings of the 5th International Conference on Mathematical Modelling* (U.C. Berkeley, Calif., July 29-31.)

Gardner, F. M. 1979. *Phaselock Techniques*. John Wiley & Sons Publishing Co., New York, N.Y.

Gardner, F. M. 1980. "Charge-Pump Phase Locked Loops." *IEEE Transactions on Communications* COM-28, no. 11 (Nov.): 1849-1858.

Mitchell, E. L. 1978. "Phase Locked Loop Techniques: Interactive Simulation With the Advanced Continuous Simulation Language (ACSL)." In *Proceeding of the 1978 Summer Computer Simulation Conference* (Newport Beach, Calif.). SCS, San Diego, Calif., 444-451.

Electrical Engineering

MONOLITHIC PHASE-LOCKED LOOPS AND CLOCK RECOVERY CIRCUITS

Theory and Design

Featuring an extensive 40-page tutorial introduction, this carefully compiled anthology of 65 of the most important papers on phase-locked loops and clock recovery circuits brings you comprehensive coverage of the field—all in one self-contained volume. You'll gain an understanding of the analysis, design, simulation, and implementation of phase-locked loops and clock recovery circuits in CMOS and bipolar technologies along with valuable insights into the issues and trade-offs associated with phase-locked systems for high speed, low power, and low noise. This authoritative volume addresses the very building blocks of phase-locked systems:

- Discrete-time and noise analysis of phase-locked loops
- Design of oscillators, phase/frequency detectors, and charge pumps
- Modeling and simulation
- Design of phase-locked loops in CMOS and bipolar technologies
- Design of clock recovery circuits for various applications

From the underlying theory to state-of-the-art applications, *Monolithic Phase-Locked Loops and Clock Recovery Circuits* is an excellent reference for design engineers, students, and researchers with an interest in solid-state circuits, circuits and systems, and consumer electronics.

Also of Interest from IEEE Press . . .

CLOCK DISTRIBUTION NETWORKS IN VLSI CIRCUITS AND SYSTEMS
edited by Eby G. Friedman
1995 Hardcover 544 pp IEEE Order No. PC4127 ISBN 0-7803-1058-6

DELTA-SIGMA DATA CONVERTERS
edited by Steven R. Norsworthy, Richard Schreier, and Gabor C. Temes
1996 Hardcover 512 pp IEEE Order No. PC3954 ISBN 0-7803-1045-4

SUCCESSFUL PATENTS AND PATENTING FOR ENGINEERS AND SCIENTISTS
edited by Michael A. Lechter
1995 Softcover 432 pp IEEE Order No. PP4478 ISBN 0-7803-1086-1

IEEE Press
445 Hoes Lane
PO Box 1331
Piscataway, NJ 08855-1331
1-800-678-IEEE

ISBN 0-7803-1149-3